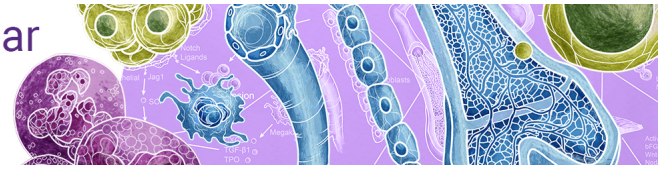

The Journal of Immunology

TCR Stimulation Drives Cleavage and Shedding of the ITIM Receptor CD31

Giulia Fornasa, Emilie Groyer, Marc Clement, Jordan Dimitrov, Caroline Compain, Anh-Thu Gaston, Aditi Varthaman, Jamila Khallou-Laschet, Debra K. Newman, Stéphanie Graff-Dubois, Antonino Nicoletti and Giuseppina Caligiuri

J Immunol 2010; 184:5485-5492; Prepublished online 16 April 2010;
doi: 10.4049/jimmunol.0902219
http://www.jimmunol.org/content/184/10/5485

The Journal of Immunology is published twice each month by
The American Association of Immunologists, Inc.,
1451 Rockville Pike, Suite 650, Rockville, MD 20852

Print ISSN: 0022-1767 Online ISSN: 1550-6606.

TCR Stimulation Drives Cleavage and Shedding of the ITIM Receptor CD31

Giulia Fornasa,* Emilie Groyer,* Marc Clement,* Jordan Dimitrov,† Caroline Compain,* Anh-Thu Gaston,* Aditi Varthaman,* Jamila Khallou-Laschet,*,‡ Debra K. Newman,§ Stéphanie Graff-Dubois,*,¶ Antonino Nicoletti,*,‡ and Giuseppina Caligiuri*

CD31 is a transmembrane molecule endowed with T cell regulatory functions owing to the presence of 2 immunotyrosine-based inhibitory motifs. For reasons not understood, CD31 is lost by a portion of circulating T lymphocytes, which appear prone to uncontrolled activation. In this study, we show that extracellular T cell CD31 comprising Ig-like domains 1 to 5 is cleaved and shed from the surface of human T cells upon activation via their TCR. The shed CD31 can be specifically detected as a soluble, truncated protein in human plasma. CD31 shedding results in the loss of its inhibitory function because the necessary *cis*-homo–oligomerization of the molecule, triggered by the *trans*-homophilic engagement of the distal Ig-like domain 1, cannot be established by CD31^{shed} cells. However, we show that a juxta-membrane extracellular sequence, comprising part of the domain 6, remains expressed at the surface of CD31^{shed} T cells. We also show that the immunosuppressive CD31 peptide aa 551–574 is highly homophilic and possibly acts by homo-oligomerizing with the truncated CD31 remaining after its cleavage and shedding. This peptide is able to sustain phosphorylation of the CD31 ITIM$_{686}$ and of SHP2 and to inhibit TCR-induced T cell activation. Finally, systemic administration of the peptide in BALB/c mice efficiently suppresses Ag-induced T cell-mediated immune responses in vivo. We conclude that the loss of T cell regulation caused by CD31 shedding driven by TCR stimulation can be rescued by molecular tools able to engage the truncated juxta-membrane extracellular molecule that remains exposed at the surface of CD31^{shed} cells. *The Journal of Immunology*, 2010, 184: 5485–5492.

CD31 (PECAM-1, Fig. 1*A*) consists of a single-chain molecule comprising 6 Ig-like extracellular domains, a short transmembrane segment, and a cytoplasmic tail containing two immunotyrosine-based inhibitory motif (ITIM) units (1). The presence of Ig-like domains and their high density at endothelial intercellular borders has previously led to the hypothesis that CD31 functions as a cell adhesion molecule (2), and experimental studies showed that CD31-specific mAbs or recombinant soluble proteins block transendothelial migration of monocytes and neutrophils (3). In contrast, in vitro (4) and in vivo (5) studies have shown that lymphocyte CD31 expression is negatively correlated with transmigration. Indeed, it has been demonstrated experimentally that *trans*-homophilic CD31 engagement drives lymphocyte detachment from APCs (6) and inhibits TCR-mediated signal transduction (7), pointing to an important immunoregulatory function for T cell CD31 surface molecules. Moreover, CD31 knockout mice are prone to develop chronic inflammatory diseases (8–10).

Previous studies have demonstrated that a subset of T cells in adult human blood, mostly within the CD45RA$^-$/CD45RO$^+$ (memory) subpopulation (11, 12), lack CD31. Furthermore, an effective loss of CD31 is observed upon lymphocyte activation and differentiation (13), especially in CD4+ T cells activated via TCR stimulation (14). Nevertheless, the mechanism underlying the loss of CD31 from the T cell surface is not known. Downregulation of the CD31 transcript has been documented in lymphocytes lacking surface CD31 (13). However, regulation of CD31 expression levels at the transcript level does not appear to be the mechanism responsible for downmodulation of CD31 expression in response to TCR stimulation, because CD31 expression is constitutive and turnover of the molecule takes 48 h (15), whereas the process of CD31 disappearance upon T cell activation takes <16 h (16). These findings indicate that another mechanism is responsible for the rapid loss of CD31 that occurs upon lymphocyte activation.

We hypothesized that CD31 could undergo proteolytic cleavage and thus escape detection via the shedding of a cleaved extracellular portion of the protein (17). This process is extremely rapid (18) and is similar to the mechanism observed with other transmembrane molecules bearing Ig-like domains (19, 20). This hypothesis is supported by the fact that plasma CD31 exists in two distinct forms: a transmembraneless form (120 kDa) and a truncated form (90 kDa). The transmembraneless form resembles the one produced by alternative splicing of the transmembrane segment-encoding (exon 9) transcript documented in endothelial and myeloid cell lines (15).

*Institut National de la Santé de la Recherche Médicale, U698; †Centre de Recherche des Cordeliers, U872; ‡Université Denis Diderot; ¶Université Pierre et Marie Curie, Paris, France; and §Blood Research Institute, Blood Center of Wisconsin, Milwaukee, WI 53201

Received for publication July 13, 2009. Accepted for publication March 12, 2010.

This work was supported in part by grants from the Fondation de France (Engt 2006-005656 and 2008-002724), the Fondation pour la Recherche Médicale (DCV20070409268), and the Agence Nationale de la Recherche (project RELATE and project BROSCI). G.F. is the recipient of a training grant from the Ministère Affaires Étrangères (Égide N°636511F) and of the Groupe de Reflexion sur la Recherche Cardio-Vasculaire et la Féderation Française de Cardiologie. E.G. is the recipient of a research grant from the Fondation pour la Recherche Médicale (FDT20071211595).

Address correspondence and reprint requests to Dr. Giuseppina Caligiuri, Institut National de la Santé de la Recherche Médicale, U698, 46 Rue Henri Huchard, F-75018 Paris, France. E-mail address: giuseppina.caligiuri@inserm.fr

Abbreviations used in this paper: CBA, cytometric bead array; MFI, mean fluorescence intensity; nd, not determined; peptide, incubation with the peptide alone (100 μg/ml) for 20 min; pervanadate, incubation with sodium pervanadate (Na_3VO_8) at 100 μM for 20 min; RU, resonance units; stim, crosslinking of CD3 molecules by a monoclonal mouse anti-human CD3ε + goat anti-mouse IgG F(ab′)$_2$ fragments; stim/cross, crosslinking of CD3 with CD31 molecules via their domain 6; stim/peptide, crosslinking of CD3 in the presence of 100 μg/ml human CD31 peptide; TIRF, total internal reflection fluorescence; TNCB, 2-chloro-1,3,5-trinitrobenzene; Unstim, membrane lysate from untreated Jurkat cells.

www.jimmunol.org/cgi/doi/10.4049/jimmunol.0902219

The truncated form (90 kDa) lacks the cytoplasmic tail (15) and could originate from proteolytic cleavage at the cell surface and shedding into the plasma of the extracellular portion of CD31. A recent study by Eugenin et al. (21) showed that the positive staining for extracellular CD31 in inflamed brain tissues of patients with HIV is only minimally colocalized with the intracellular portion of CD31. The authors therefore suggested that activated inflammatory cells undergo an active shedding of extracellular CD31 which could thus contribute to the rise in soluble CD31 in the circulation of patients with inflammatory diseases (21).

In addition to the potential diagnostic value of measuring the cleaved moiety, the loss of CD31 on peripheral T cells caused by shedding, rather than its total absence, could also provide an important therapeutic potential. In this study, we show that the remaining cell surface fragment can indeed be engaged in interactions with a homotypic synthetic peptide in the aim of restoring the physiologic functions of the molecule and controlling Ag-induced T cell responses in vivo.

Materials and Methods

Assessment of CD31^{+} and CD31^{shed} peripheral blood leukocytes

Ten-color flow cytometry was performed on peripheral blood leukocytes obtained from five healthy individuals. The leukocytes were either maintained in basal conditions or stimulated overnight with soluble purified anti-CD3 Ab (R&D Systems Europe, Lille, France) at 1 μg/ml. Cells were fixed in PBS/formaldehyde 1%/FCS 1% for 4 min at 37°C and subjected to erythrocyte hypotonic lysis (10 min at 37°C 1:10 v/v in Tris 10 mM, NH_4Cl 155 mM, $KHCO_3$ 10 mM, pH 7.4), prior to processing. All experiments on human samples were approved by the Institutional Ethical Committee (www.clinicaltrials.gov; Identifier: NCT00430820). Pelleted cells were incubated for 30 min at room temperature and protected from light, with a mixture of fluorescent mAbs directed toward CD4 (PE-Cy7), CD8 (PerCP), HLA-DR (APC-Cy7), CD45RA (Pacific Blue), CD14 (APC), CD10 (PE-Cy5), and CD31 (clone WM59, PE) from BD Biosciences (San Jose, CA) and CD3 (PE-Texas Red), CD20 (AlexaFluor700), and CD31 (clone MBC 78.2, FITC) from Invitrogen (Cergy Pontoise, France). At least 50,000 events were acquired in the lymphocyte gate using a BD LSRII equipped with three lasers (405, 488, and 633 nm) and analyzed with BD FACSDiva 6.0 software (BD Biosciences, Le Pont de Claix, France).

Subtractive measurement of soluble CD31 (Patent No. PCT/EP2009/058220)

To detect the soluble or solubilized CD31 forms containing the Ig-like domain 1 and/or 2 and/or 5 and/or 6, we have customized the cytometric bead array (CBA; BD Biosciences) technology. Functional CBA beads were coupled with purified monoclonal anti-CD31 Abs against either the most distal Ig-like domain 1 (clone JC70A; Dako (22) or the most proximal Ig-like domain 6 (clone MBC 78.2) (23), also known as PECAM-1, provided by Dr. Peter Newman (Milwaukee Blood Center, Milwaukee, WI). The coupled beads (Fig. 2) were incubated with the plasma of healthy subjects, culture supernatant, and membrane lysates from stimulated Jurkat cells and serial dilutions of the standard (recombinant, full length extracellular CD31, aa 1–574; R&D Systems). Positive binding of circulating CD31 captured by the anti-CD31 cytometric beads was detected by a combination of three anti-CD31 mAbs directed against Ig-like domain 2 (clone WM-59, PE from BD Biosciences) (22), domain 5 (clone HC1/6, FITC from Invitrogen) (22) and domain 6 (clone MBC 78.2 coupled to Pacific Blue using the kit #P30013 from Invitrogen) (23). The median fluorescent intensity of each detecting Ab was analyzed on ≥1000 acquired beads. The three standard curves were obtained by using all detecting Abs simultaneously on the serial dilutions of recombinant CD31 to overcome any bias caused by differences in binding affinity of the diverse Abs. The concentration of soluble CD31 forms comprising at least domain 1–2 (capture by JC70A, detection by WM59-PE), domain 1–5 (capture by JC70A, detection by HC1/6-FITC) domain 1–6 (capture by JC70A, detection by MBC 78.2-Pacific Blue), domain 6 (capture by MBC 78.2, detection by MBC 78.2-Pacific Blue), domain 5–6 (capture by MBC 78.2, detection by HC1/6), or domain 2–6 (capture by MBC 78.2, detection by WM59) of CD31 in samples was calculated using the linear regression formula obtained with the same capture beads and detecting Abs on the serial standard dilutions. In plasma and culture supernatant, the concentration of CD31 domain 1–6 was subtracted from the concentration of CD31 domain 1–5 to obtain the amount of truncated CD31 lacking domain 6. The latter was subtracted from the concentration of CD31 domain 1–2 to calculate the value of soluble CD31 lacking both domains 5 and 6. In membrane lysates, the concentration of CD31 domain 2–6 was subtracted from the concentration of CD31 domain 5–6 to obtain the fraction lacking at least domain 2. The concentration of CD31 Δ2 was then subtracted from CD31 domain 6 to obtain the fraction lacking both domains 2 and 5.

Peptides

The human (NHASSVPRSKILTVRVILAPWKK, MW 2601.2) and the mouse (SSMRTSPRSSTLAVRVFLAPWKK, MW 2606.0) custom peptides were synthetized by Genosphere (Paris, France) and by Mimotopes (Clayton, Victoria, Australia). The 5(6)-FAM human sequence was provided by Mimotopes. Peptides were >95% pure, as assessed by analytical reverse phase HPLC, and were checked for correct identity by amino acid analysis and mass spectrometry. Upon receipt from the fabricant, the lyophilized peptides were dissolved in sterile PBS/DMSO and the concentration was determined by UV spectroscopy at 280 nm. Endotoxin levels were consistently <0.01 ng/μg of peptide as determined by the LAL test. The peptide stock concentration was adjusted to 10 mg/ml with sterile PBS (final concentration of DMSO ≤5%) and stock aliquots were stored at −20°C in a manual defrost freezer.

Total internal reflection fluorescence microscopy

Freshly purified CD4^{+} cells from heparinized peripheral blood obtained by positive magnetic selection (Dynabeads FlowComp Human CD4 kit; Invitrogen) were stimulated by CD3 crosslinking as described under *TCR stimulation in vitro* in the presence of either 100 μg/ml unlabeled human CD31 peptide, 100 μg/ml 5,6 FAM human CD31 peptide or 10 μg/ml CD31 domain 6 Ab (clone MBC 78.2) directly coupled to AlexaFluor546 (mAb Labeling Kit #A-20183; Invitrogen). Unstimulated cells and cells stimulated for 20 min were plunged immediately into one volume of ice-cold 2% paraformaldehyde for 15 min. Cells were subsequently pelleted and resuspended in 2% paraformaldehyde for an additional 15 min on ice. Following fixation, the cells were rinsed three times in 1× PBS and incubated overnight at room temperature with 10 μg/ml AlexaFluor546 CD31 domain 6 (clone MBC 78.2), as appropriate. After incubation, cells were washed twice, postfixed with 1% paraformaldehyde, and transferred to 35-mm glass-bottom poly-D-lysine coated dishes (#P35GC-1.5-10-C; MatTek, Ashland, MA) and left to adhere for 2 h in PBS. Three independent experiments gave similar results. Digital images were acquired using the objective PLAPO 100xO TIRFM (NA 1.45) on an Olympus IX81 (Melville, NY) inverted microscope equipped with a total internal reflection fluorescence microscopy module (488 and 561 nm) and a cooled monochromatic digital camera (EMCCD DU885 iXon+, Andor, South Windsor, CT) and were subsequently analyzed using ImageJ software (National Institutes of Health freeware, http://rsbweb.nih.gov/ij/).

Plasmon surface resonance

Homophilic peptide association and dissociation were evaluated in three independent experiments by surface plasmon resonance (BIAcore 2000; GE Healthcare, Saclay, France). Human and murine peptides were amine-coupled (2000–5000 resonance units [RU]) to CM5 chips according to the manufacturer's instructions. For the kinetic measurements, six 2-fold concentrations of the same peptides (concentration range from 0.625 to 20 μg/ml) in 10 mM HEPES pH 7.4, 140 mM NaCl, 3 mM EDTA, 0.005% Tween 20 were injected over the chip surface at a flow rate of 10 μl/min at 25°C. The BIAevaluation 3.0 Software (GE Healthcare) was used for evaluation and data are expressed as ΔRU (RU on the peptide-coated channel minus RU on the channel coated with a control, scrambled peptide). The rate equation used for the analysis was a 1:1 binding with drifting baseline model.

TCR stimulation in vitro

For T cell activation, human PBMCs or spleen cells from CD31$^{+/+}$ and CD31$^{-/-}$ mice (C57BL/6 background; The Jackson Laboratory, Bar Harbor, ME) were stimulated in vitro as previously described (24). Cells were plated in triplicate at 0.2×10^6 cells/well in a U-bottom 96-well plate in complete medium (RPMI 1640, 1% pyruvate, 1% glutamine, 1% penicillin-streptomicyn-fungizone, 10% decomplemented FCS; Invitrogen) containing 1 μg/ml anti-mouse CD3/CD28 or 5 μg/ml anti-human CD3 Abs (BD Biosciences) as appropriate. Human or mouse CD31 peptide at 25, 50, and 100 μg/ml and scrambled peptide at 100 μg/ml final concentration were deposited in the wells just before cell plating. For T cell proliferation analysis, plated cells were cultured for 72 h in 5% CO_2 at 37°C. [^{3}H]Thymidine (0.5 μCi/well) was added for the last 16 h, and

proliferation was evaluated using a Tomtec harvester (Tomtec, Hamden, CT) and analysis on a Wallace micro β counter (Perkin Elmer, Waltham, MA). Each condition was performed in triplicate, and the experiments were repeated three times. The same conditions of culture were tested to determine the amount of apoptotic cells at 36 h using annexin V and 7-AAD staining. Cells were acquired using a BD LSRII and analyzed with BD FACSDiva 6.0 software (BD Biosciences). Data obtained from six independent experiments yielded similar results.

Assessment of CD31 pY686 (Patent No. PCT/EP2009/058220) and SHP2 pY542

Log-phase Jurkat cells (10^7 cells per condition) were stimulated to induce PECAM-1 tyrosine phosphorylation and SHP-2 binding. Cell suspensions (1 ml) were incubated with no Ab, with a human CD3ε-specific Ab (clone UCTH1, 1 μg/ml; R&D Systems) alone, or in the presence of a human CD31-specific Ab directed to domain 6 (MBC 78.2, 50 μg/ml) (23) or human CD31 peptide (100 μg/ml) for 30 min on ice. To remove unbound Abs, cells were washed twice with 5 ml ice-cold 0.145 M NaCl, BSA 0.1%, 10 mM HEPES, 2.8 mM KCl, 2 mM $MgCl_2$, 10 mM D-glucose, and 10 mM $CaCl_2$ and then resuspended in the same buffer to a final concentration of 2×10^7 cells/ml. The washing step was omitted for CD31 peptide conditions. To induce the crosslink reaction, cells were prewarmed for 10 min at 37°C, and then goat anti-mouse IgG $F(ab')_2$ fragments (The Jackson Laboratory) were added to achieve a final concentration of 20–100 μg/ml. At the specified time points, cells were rapidly spun and the supernatant was replaced by an equal volume of lysis buffer (50 mM Tris, 150 mM NaCl, 1% Triton X-100 [pH 7.4], 1× protease inhibitor mixture Sigma #P-8340, 1× phosphatase inhibitor mixture-2 Sigma #P-5726). Lysis was performed on ice for 30 min. Control conditions included cells either left unstimulated (negative control) or incubated with sodium pervanadate (Na_3VO_8, positive control). The last control consisted of unstimulated cells incubated with the peptide alone. Lysates were ultracentrifuged, and the supernatant was aliquoted and stored at −80°C until analysis. Lysates (20 μl per condition) were each incubated with Functional CBA beads (BD Biosciences) coated with an mAb directed to the PECAM-1 C-terminal sequence (clone 235.1; provided by Dr. Peter Newman) for 3 h at room temperature. Beads were subsequently washed with CBA washing buffer (BD Biosciences) and incubated with 2 μl undiluted rabbit anti-CD31 phospho-tyrosine 686 (pY686) sera (provided by Dr. Peter Newman). This step was followed by two washing steps and further incubation with AlexaFluor488-conjugated $F(ab')_2$ fragments (2 μg/ml in CBA washing buffer) of goat anti-rabbit IgG (Invitrogen). For quantifying pSHP2, cells were stimulated as described above. At the same time points as above, the cells were fixed with BD Cytofix Buffer for 10 min at 37°C, permeabilized with BD Phosflow Perm Buffer III on ice for 30 min, and blocked with normal mouse immunoglobulin, followed by intracellular staining using 2 μl undiluted PE mouse anti-SHP2 (pY542) Ab (clone L99–921; BD Biosciences). Each condition was performed in triplicate, and the experiments were repeated three times. The beads (>1000 per condition) and cells (10^6 per condition) were analyzed on an LSRII cytometer (BD Biosciences) in the 530/30 nm (pY686) and 575/26 nm (pY542) detection channel. Data are expressed as median fluorescence intensity (MFI) calculated with the FACSDiva 6.0 software (BD Biosciences).

Calcium mobilization assay

Spleen cells from C57BL/6 mice were prepared as described (24). Cells were incubated with Fluo-3AM (Invitrogen, #F1242), per the manufacturer's instructions. Fluorescence of calcium-bound tracer was measured in the 530/30 nm detection channel on an LSRII cytometer (BD Biosciences). Data were acquired before and during 60 s following the addition of rat anti-mouse CD3/CD28 mAbs (10 μg/ml each; Biolegend, San Diego, CA) and Fab fragments of affinity purified goat anti-rat immunoglobulins (1.3 μg/ml; Jackson ImmunoResearch Laboratories, West Grove, PA). Measurements were taken as described above and in the presence of either rat anti-mouse CD31 Ab (clone 390, 10 μg/ml; BD Biosciences) or mouse CD31 peptide (100 μg/ml). Negative controls included rat IgG isotype control and scrambled peptide. Experiments were repeated three times and gave similar results.

Immunosuppressive effect of the peptide in vivo

Delayed type hypersensitivity suppression was evaluated as described (25). 2-Chloro-1,3,5-trinitrobenzene; Fluka #79874) was dissolved in acetone/olive oil (1:1 v/v) at a concentration of 10 mg/ml. BALB/c mice ($n = 6$ per group) were primed by painting shaved regions of the abdomen with 0.2 ml of the preparation. The experiment included three dose groups for the CD31 peptide (25, 50, 100 μg) and one for the scrambled peptide (100 μg). Five days after priming, 10 μl of the 2-chloro-1,3,5-trinitrobenzene-solvent mixture was painted on the right pinna, 30 min after s.c. (interscapolar) administration of the mouse, CD31 peptide or the scrambled peptide diluted in 100 μl PBS. Right ear thickness was measured at 24 h with a dial caliper (Pocotest; Kroeplin Längenmesstechnick, Schlüchtern, Germany). Measurement was performed five times and individual data are shown. The experience was repeated three times and gave similar results.

Statistical analysis

Data are expressed as mean ± SEM unless indicated otherwise in the text. Differences between paired experimental conditions were analyzed by Student t test and were considered statistically significant at $p < 0.05$.

Results

A portion of the membrane proximal extracellular CD31 is always present at the surface of blood lymphocytes

To establish whether the loss of CD31 was restricted only to a part or extended to the totality of its six extracellular Ig-like domains, we have performed multicolor flow cytometry analysis of peripheral blood leukocytes from five healthy donors. We used two different CD31 Abs specifically recognizing either the membrane-distal Ig-like domain 2 [clone WM59, defined in *Leucocyte Typing VI* and Fawcett et al. (22)] or the membrane-proximal Ig-like domain 6 [clone MBC 78.2/PECAM-1.2 (23); Fig. 1*A*]. We have simultaneously used a panel of lineage markers as well as the expression of CD45RA and HLA-DR. Most $CD14^+$ (monocytes) and $SSC^{high}CD10^+$ (granulocytes) cells were positively detected by both CD31 mAbs (data not shown). However, a variable portion of $CD3^+$ (T) and $CD20^+$ (B) lymphocytes were $WM59^-$ and therefore lacked at least the membrane-distal Ig-like domains 1 and 2 of the CD31 molecule (data not shown). $CD4^+CD3^+$ T cells displayed the highest fraction of $WM59^-$ lymphocytes (≥30%), which increased dramatically from naive ($CD45RA^+$) to memory ($CD45RA^-$) cells (Fig. 1*B*). Recently activated ($CD45RA^-$ $HLA\text{-}DR^+$) lymphocytes were virtually all $WM59^-$ (data not shown). All of these cells, however, expressed at least the portion of the membrane-proximal Ig-like domain 6 of CD31, regardless of their state of maturation or activation (Fig. 1*B*).

Loss of the domain 2 of CD31 could be experimentally induced by Ab-mediated TCR engagement. This led to a shift in phenotype of >80% of the peripheral blood resting T cells from CD31 $WM59^+$/MBC 78.2^+ to $WM59^-$/MBC 78.2^+ phenotype (Fig. 1*C*).

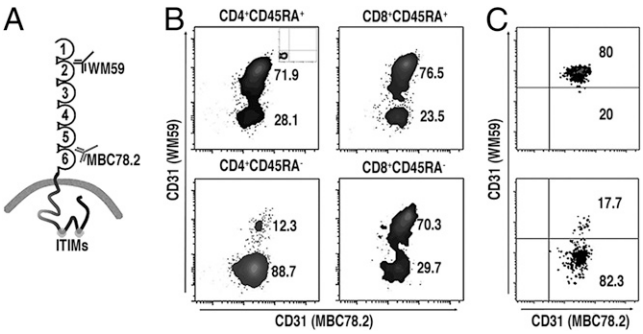

FIGURE 1. Flow cytometric analysis of CD31 expression on blood leukocytes. *A*, Schematic representation of membrane-bound CD31 and of the mAbs used to detect the CD31 domains 2 (WM59) and 6 (MBC 78.2) on peripheral blood leukocytes. *B*, Representative example of flow cytometric analysis of human peripheral blood cells from a healthy donor. $CD8^+$ and $CD4^+$ subpopulations were gated within $CD3^+$ cells and were analyzed for the expression of CD45RA. The proportion of cells lacking domain 2 was dramatically increased in memory ($CD45RA^-$) cells compared with naive ($CD45RA^+$) cells. All leukocytes were positive for CD31 domain 6. Isotype controls of WM59 and MBC 78.2 Abs are shown in the insets. *C*, Fresh peripheral blood-derived resting $CD4^+$ T cells (*top*) lost their CD31 domain 2 upon TCR activation (*bottom*).

Truncated CD31 lacking the membrane-proximal extracellular domain 6 accumulates in human plasma and in the supernatant of activated T cells

We prepared an assay to enable the discrimination between soluble CD31 molecules containing or lacking domain 6, by subtraction. Domain 6, which is normally present on all peripheral blood leukocytes, should be missing from the plasma CD31 formed after cleavage and shedding from cells (Fig. 1*B*, 1*C*). Alternatively, domain 6 should still be present in the soluble CD31 form after splicing (15). We used cytometric beads and a combination of fluorescent-specific mAbs that map to the different CD31 domains: domain 1 (clone JC70A) (22), domain 2 (clone WM59) (22), domain 5 (clone HC1/6) (22), and domain 6 (clone PECAM-1.2/MBC 78.2) (23). We found that the plasma of healthy donors ($n = 12$) contained 12.87 ± 0.89 ng/ml of soluble CD31 molecules, comprising at least Ig-like domains 1 and 2. A fraction of plasma CD31 (6.69 ± 2.10 ng/ml) contained all the six extracellular Ig-like domains. This fraction, detected by both JC70A (domain 1) and MBC 78.2 (domain 6) mAbs, likely corresponds to the spliced transmembraneless plasma CD31 (15). A smaller fraction (6.18 ± 2.36 ng/ml) of plasma CD31 failed detection by MBC 78.2 mAb (domain 6), but was detected to a large extent (≥76%) by HC1/6 mAb (domain 5). Only a minimal fraction (1.43 ± 0.91 ng/ml) of plasma CD31 was detected by the WM59 Ab (domain 2), whereas it was undetectable by both MBC 78.2 (domain 6) and HC1/6 (domain 5) Abs.

To assess whether CD31 extracellular cleavage and shedding was linked to the activation of T cells, we stimulated Jurkat cells by CD3 crosslinking for 0, 5, and 20 min. We then analyzed the integrity of CD31 molecules in both the supernatant and the cell lysate (membrane proteins). For this purpose, the immunosubtractive analysis was based on the capture of CD31 membrane-distal (supernatant) or membrane-proximal (membrane lysate) Ig-like domains by cytometric beads and simultaneous detection of the other Ig-like domains by a mixture of three fluorescent mAbs (Fig. 2). The soluble CD31 molecule concentration in the supernatant (comprising at least Ig-like domains 1 and 2) increased dramatically 5 min after T cell stimulation (from 1.61 ± 0.05 to 6234 ± 323 ng/ml) and kept increasing up to 20 min (7507 ± 538 ng/ml) after stimulation. Most (86–88%) of the soluble protein also comprised the Ig-like domain 5 but lacked domain 6 (Fig. 2). In parallel, >99% of the T cell-bound CD31 molecules captured via the detection of domain 6 lacked both Ig-like domains 5 and 2 (Fig. 2).

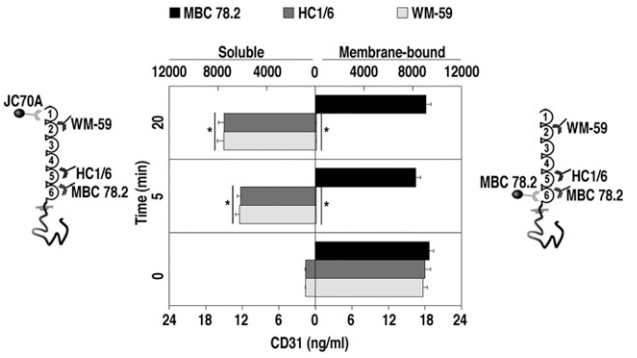

FIGURE 2. Analysis of soluble and membrane-bound CD31 upon T cell activation. Results from six independent experiments are shown in the mirrored bar histograms. Soluble CD31 (*left panel*) and membrane-bound CD31 (*right panel*) were measured, respectively, in the supernatant and in membrane lysates of Jurkat cells stimulated via their TCR by cross-linking CD3 molecules, as previously described (7). Supernatant and membrane lysates were collected at 0, 5, and 20 min after TCR stimulation. For supernatant analysis, CD31 molecules were captured by cytometric beads coupled to JC70A Abs (domain 1). For membrane lysates, the capture was performed with cytometric beads coupled to MBC 78.2-Abs (domain 6). CD31 molecules captured by either type of bead were revealed using a three-color CD31 Ab mixture (WM59-domain 2 coupled to PE, HC1/6-domain 5 coupled to FITC, and MBC 78.2 couped to Pacific Blue). The same sets of capture and detecting Abs were used to obtain the standard curves using serial dilutions of recombinant human CD31. Data are expressed as nanograms per milliliter. Before TCR stimulation ($t = 0$), soluble CD31 is virtually absent in the supernatant, while all three detecting Abs are able to detect membrane-bound CD31 molecules. Upon TCR stimulation at 5 and 20 min, virtually all CD31 molecules are cleaved upstream of the epitope recognized by MBC 78.2 (domain 6) Abs, because these are the only Abs that are able to reveal the membrane-bound CD31 molecules at these time points. The missing fragment comprising domain 1 (capture by JC70A) and domain 2 (detection by WM59) through to domain 5 (detection by HC1/6) is shed from the membrane and detected in the supernatant. Bottom *x*-axis applies to $t = 0$; the top *x*-axis applies to times 5 and 20 min.

A peptide homotypic of the residual extracellular CD31 fragment on CD31^{shed} T cells rescues the CD31 ITIM/SHP2 inhibitory pathway

A CD31 domain-6–derived synthetic peptide, corresponding to the 23 juxta-membrane positioned amino acids of the extracellular human CD31 sequence (NHASSVPRSKILTVRVILAPWKK) (26), showed a dose-dependent suppressor effect on the proliferation of human peripheral blood T cells stimulated in vitro by using anti-CD3ε Abs (Fig. 3*A*). The antiproliferative effect of the peptide did not correlate with its proapoptotic effect, which was minimal (data not shown). Surface plasmon resonance (BIAcore, GE Healthcare) analysis demonstrated that this peptide is homophilic (Fig. 3*B*). The BIAcore curves followed concentration-dependent association and dissociation models of the peptide over its homotypic sequence. At low concentrations (≤1.25 μg/ml), the curves showed steady values of ΔRU over time (Fig. 3B) following a 1:1 binding (homodimerization) model. At >2.5 μg/ml, the curves showed increasing ΔRU values during the association phase and did not drop to baseline upon peptide washout indicating a >1:1 binding (homo-oligomerization) model. For the analysis, different binding models (different rate equations) were tested in the global curve fitting procedure. The model best describing the experimental data were a 1:1 binding with a drifting baseline model. However, this model could be applied only to low concentrations of the analyte (≤1.25 μg/ml). At concentrations >2.5 μg/ml, the BIAcore curves suggest peptide polymerization, implying that peptide monomers are in equilibrium with peptide dimers, trimers, and tetramers. As a consequence, it was not possible to evaluate the association and dissociation constants of the peptides at the biologically active concentrations (≥10 μg/ml) that have been used in our experiments.

To assess whether the homophilic peptide could engage the signaling of CD31 despite its shedding, we evaluated the level of phosphorylation of the CD31 ITIM tyrosine at position 686 and of the SHP2 tyrosine at position 542 in stimulated Jurkat cells (Fig. 3*C*, 3*D*). Crosslinking of CD3ε alone induced a discrete increase in CD31 pY686, relative to the unstimulated control. However, the presence of CD31 Ab directed against domain 6 or of the CD31 peptide (Fig. 3C) during the first 5 min of stimulation induced a higher level of CD31 pY686 phosphorylation. After 20 min of stimulation, phosphorylation was further increased in the presence of the CD31 peptide. In parallel, the peptide treatment led to a significant and durable increase in intracellular SHP2 Y542 phosphorylation induced by CD3ε cross-linking (Fig. 3*D*), which was comparable to that obtained by Ab-mediated CD31 domain 6 crosslinking. The peptide alone did not change either tyrosine-phosphorylation levels as compared with unstimulated cells (Fig. 3*C*, 2*D*).

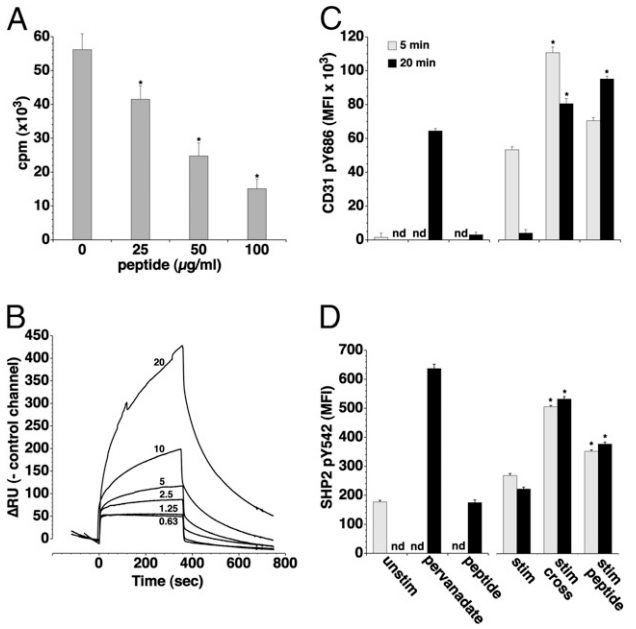

FIGURE 3. A homophilic peptide derived from the residual extracellular fragment on $CD31^{shed}$ inhibits T cell activation and rescues CD31 signaling. *A*, Proliferative response to TCR engagement of human PBMCs in the presence of increasing doses of human CD31 peptide. $*p < 0.05$ versus dose 0. CD31 peptide inhibits cell proliferation in a dose-dependent manner. *B*, Real-time (BIAcore) analysis of the human CD31 peptide homophilic interaction at 2-fold stepwise dilutions of the peptide (0.63, 1.25, 2.5, 5, 10, and 20 μg/ml). Data are normalized regarding the control channel (scrambled peptide) and expressed as ΔRU. *C* and *D*, Flow cytometric assessment of human CD31 pY686 (*C*) and of SHP2 pY542 (*D*) on cultured Jurkat cells. Quantification of CD31 pY686 was performed on solubilized membrane-bound CD31. SHP2 pY542 was analyzed by intracellular staining. Data are expressed as MFI. The cross-linking of the TCR alone and with CD31 molecules induces a rapid and transient phosphorylation of the CD31 inhibitory motifs, whereas the peptide treatment is able to sustain phosphorylation for at least 20 min after stimulation ($*p < 0.001$, between stim peptide and stim at 20 min). In parallel, the peptide increases the SHP2 Y542 phosphorylation to an extent comparable with that observed with CD31 Ab-mediated crosslinking ($*p < 0.001$, between stim peptide and stim). Peptide, incubation with the peptide alone (100 μg/ml) for 20 min; pervanadate, incubation with sodium pervanadate (Na_3VO_8) at 100 μM for 20 min; stim, crosslinking of CD3 molecules by a monoclonal mouse anti-human CD3ε + goat anti-mouse IgG $F(ab')_2$ fragments; stim/cross, crosslinking of CD3 with CD31 molecules via their domain 6; stim/peptide, crosslinking of CD3 in the presence of 100 μg/ml human CD31 peptide; unstim, membrane lysate from untreated Jurkat cells.

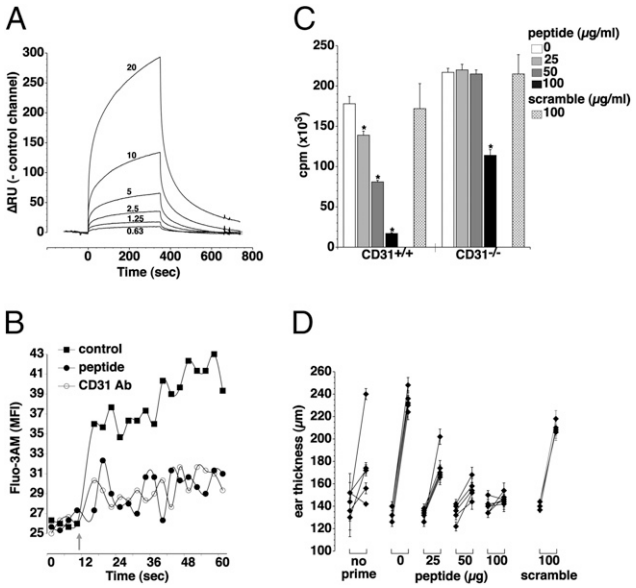

FIGURE 4. The mouse equivalent of the CD31 homotypic peptide inhibits T cell responses in vitro and in vivo. *A*, BIAcore analysis of the mouse CD31 peptide homophilic interaction at different concentrations (0.63, 1.25, 2.5, 5, 10, and 20 μg/ml). Real-time binding is evaluated as for the equivalent human CD31 peptide detailed in Fig. 3. Data are normalized against the control channels and expressed as ΔRU. *B*, Intracellular calcium mobilization induced by crosslinking of mouse CD3ε and CD28, determined by flow cytometry in Fluo-3AM–loaded spleen cells. Data are expressed as MFI detected in the FITC channel (BP 530/30 nm). The gray arrow indicates the addition of anti-CD3/CD28 Abs and the cross-linker alone (■ = control) or together with either mouse CD31 peptide at 100 μg/ml (●) or CD31 Ab, clone Mab390 (○). The peptide treatment inhibits, upon TCR stimulation, the intracellular calcium influx to the same extent as CD31 crosslinking. *C*, Inhibitory effect of the mouse peptide on the proliferative response of $CD31^{+/+}$ and $CD31^{-/-}$ spleen cells. The cross-hatched column shows 100 μg/ml of the scrambled peptide. $*p < 0.05$, versus previous peptide dose. *D*, Immunosuppressive effect of the mouse peptide in vivo on a model of delayed type hypersensitivity. Mice were treated with different doses of the peptide (0, 25, 50, 100 μg) or with a scramble peptide (100 μg). The graphic shows individual right ear thickness (average of 5 measurements ± SEM) of each mouse, before and 24 h after elicitation. The control group of mice did not receive the priming (no prime).

Mouse CD31 peptide 551–574 binds to the homotypic sequence and inhibits lymphocyte activation in vitro and in vivo

To further test our hypothesis, it was necessary to perform in vivo experiments; therefore, we synthesized the murine equivalent of CD31 (551–574) peptide (NH2-SSMRTSPRSSTLAVRVFLAPWKK-COOH) and evaluated its properties in vitro and in vivo. As the human equivalent, the murine CD31 peptide showed consistent homophilic interaction, as analyzed by surface plasmon resonance (Fig. 4*A*). In response to the coengagement of CD3 and of the costimulatory molecule CD28 in spleen lymphocytes, the peptide was able to inhibit calcium mobilization to the same extent as CD31 cross-linking by specific mAbs (Fig. 4*B*). Furthermore, the peptide inhibited the proliferation of spleen cells in a dose-dependent manner in response to stimulation of the T cell receptor in vitro. At low doses, the effect of the peptide was exclusively due to its homophilic binding with CD31 molecules, because no effect was observed on spleen cells from $CD31^{-/-}$ mice. However, at high concentrations, the peptide can also bind to other (low-affinity) heterophilic ligands, as suggested by its effect at a 100-μg/ml dose on cells lacking CD31. The scrambled peptide (NH2-SMPAVRSRF SATSLVTLKSRWPK-COOH), used at the highest dose, was ineffective on both $CD31^{+/+}$ and $CD31^{-/-}$ cells (Fig. 4*C*). The immunosuppressive effect of the peptide was also documented in vivo, using a model of delayed type hypersensitivity. In this model, the antigenic challenge is first exerted over the abdominal skin, and the response is easily quantified after a second challenge 1 wk later by measuring the thickness of the pinna of the ear (Fig. 4*D*). The effect of the treatment was calculated as percent suppression = $(1 - \Delta TE / \Delta TS) \times 100$, where ΔT = (ear thickness 24 h after elicitation) – (baseline ear thickness), E = sensitized animals, and S = treated animals (25). A minor reduction of the ear thickness (33 ± 4%) was observed in the mice treated with 100 μg of the scrambled peptide. The injection of 25, 50, and 100 μg of peptide prior to the elicitation inhibited the delayed type hypersensitivity response by 48 ± 5% ($p < 0.05$ versus scrambled), 80 ± 4% ($p < 0.001$ versus scrambled), and 90 ± 3% ($p < 0.001$ versus scrambled), respectively; n = 6 mice per group.

Peptide treatment affects surface CD31 redistribution and clustering upon TCR stimulation

To evaluate whether the peptide acts by homo-oligomerization with the truncated CD31, we observed the CD31 redistribution on the membrane of TCR-stimulated cells by immunostaining the domain 6 of the molecule and total internal reflection fluorescence (TIRF) microscopy. This technique allows high-resolution visualization of processes that occur in the cell membrane. CD31 molecules, which were homogeneously distributed on the surface of unstimulated cells (Fig. 5*A*), showed a modest redistribution and cluster formation upon TCR stimulation (Fig. 5*B*). The crosslinking of TCR with the CD31 slightly increased cluster formation as compared with TCR stimulation alone (Fig. 5*C*), whereas the peptide treatment led to larger clusters (Fig. 5*D*). To visualize the localization of the peptide, we have treated the cells with a fluorescent peptide in parallel conditions. Analysis of the fluorescence intensity profiles on lines drawn across the cell membrane showed that the peptide oligomerizes and localizes within CD31 clusters, as suggested by the shift of the two fluorescence profiles (Fig. 6*E*, 6*F*).

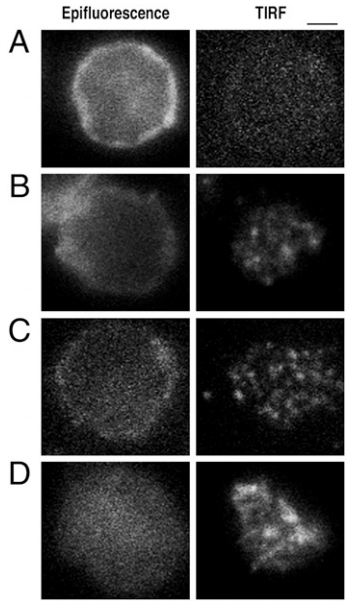

FIGURE 5. Peptide treatment affects surface CD31 redistribution and clustering upon TCR stimulation. Epifluorescence and TIRF analysis of CD31 domain 6 membrane distribution on $CD4^+$ T cells isolated from peripheral blood. Cells were either were left in basal conditions (*A*) or stimulated by crosslinking the CD3 (*B*) in the presence of 10 μg/ml anti-CD31 domain 6 Ab (clone MBC 78.2) directly coupled to AlexaFluor546 (*C*) or 100 μg/ml human CD31 peptide (*D*). After 20 min, all cells were fixed and rinsed. For the conditions *A*, *B*, and *D*, cells were stained with anti-CD31 domain 6 Ab (clone MBC 78.2) AlexaFluor546-conjugated. Cells were then transferred to poly–D-lysine–coated glass-bottom dishes, and CD31 membrane clustering was visualized by TIRF. Ab-mediated cross-linking of the CD31 domain 6 (*C*) did not change the appearance of the clustering spots as compared with T cell stimulation alone (*B*). TIRF analysis of the cells stimulated in the presence of the peptide (*D*) showed larger clustering spots. Scale bar, 5μm.

Discussion

Experimental studies have shown previously that the CD31 inhibitory pathway mediated by the ITIMs is engaged during T cell responses elicited by TCR stimulation (7). We have recently shown that the lack of T cell CD31 signaling favors autoimmune responses in vitro and in vivo (24, 27), supporting a T cell regulatory role for this transmembrane ITIM-bearing receptor (1). In this study, we show that TCR stimulation drives the cleavage and shedding of the extracellular T cell CD31 comprising Ig-like domains 1 to 5. We also show that the immunosuppressive CD31 peptide aa 551–574 (26, 28) is highly homophilic and probably acts by homo-oligomerizing with the truncated CD31 remaining after its cleavage and shedding.

Although CD31 is known to interact with heterophilic ligands on blood and vascular cells (29–32), the original feature of CD31 signaling resides in its *trans*- and *cis*-homophilic nature. According to the model proposed by Newton et al. (33), a low-affinity *trans*-homophilic engagement of the distal domains is necessary to drive the *cis*-homodimerization of the membrane-proximal portion of the molecule. This step, in turn, would be critical for triggering the phosphorylation of the ITIMs, and the recruitment and activation of SH2-containing phosphatases. This hypothesis is supported by the fact that cross-linking of the CD31 molecule is necessary to induce the phosphorylation of ITIMs (34, 35) and inhibition of Ag-driven T cell activation (7).

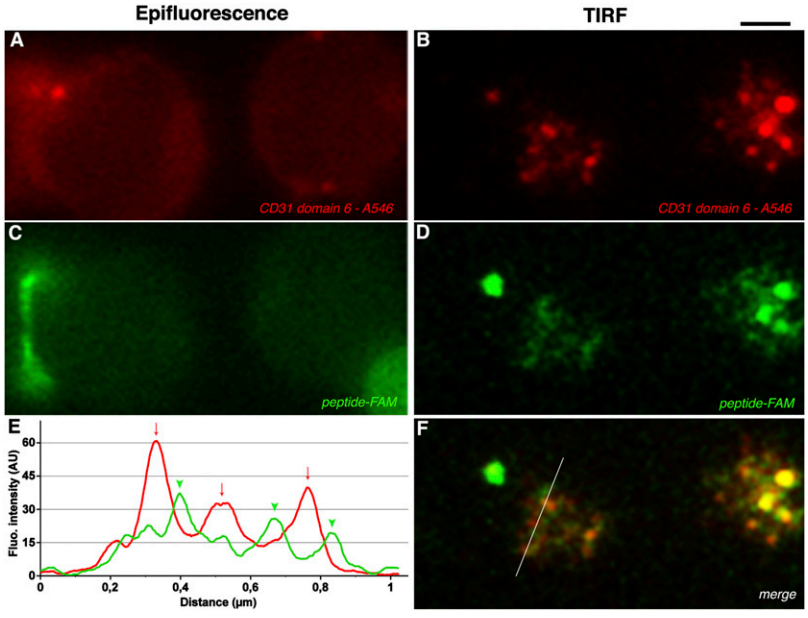

FIGURE 6. The CD31 peptide clusters on the plasma membrane, and it accumulates between CD31 clusters upon TCR stimulation. Epifluorescence and TIRF analysis of CD31 domain 6 (*A*, *B*) and of CD31 fluorescent peptide (5,6 FAM; *C*, *D*) distribution on the $CD4^+$ T cell membrane. Cells were isolated from peripheral blood and stimulated by cross-linking the CD3 molecules in presence of 100 μg/ml 5,6 FAM human CD31 peptide. Twenty minutes after stimulation, cells were fixed, rinsed, and stained with anti-CD31 domain 6 Ab (clone MBC 78.2) AlexaFluor546-conjugated. *F*, Merger of *B* and *D*. *E*, Example of the analysis of fluorescence intensity profiles obtained by line-scans across the cell in the red and green channels. The *x*-axis is the scanning coordinate in micrometers, and the *y*-axis plots the fluorescence intensities in arbitrary units. Upon TCR stimulation, the CD31 domain 6 and the CD31 human peptide form clusters on the plasma membrane (*B*, *D*) and, as shown in *E*, CD31 domain 6 clusters (arrows, red line) localize next to and in alternation with peptide clusters (arrow heads, green line). Scale bar, 5 μm.

CD31 expression is constitutive, but peripheral blood T cells of the memory–activated phenotype lack this molecule at their surface (11, 13). We demonstrate in this study that the assumption that CD31 molecules are absent on activated T lymphocytes is based on incomplete information. Indeed, the observed loss is due to a cleavage and shedding of the extracellular CD31 comprising domains 1–5. Because the membrane-proximal 6th domain remains anchored to all peripheral blood T lymphocytes, we propose to use the term *CD31^{shed}* rather than *CD31 negative cells* for the designation of lymphocytes that are not detected by mAbs directed toward the distal CD31 Ig-like domains. CD31 shedding occurs rapidly upon T cell activation and leads to an accumulation of the truncated molecule in the supernatant. The same truncated form of CD31 is also specifically detected in human plasma and could serve as a biomarker of pathologic T cell activation.

We propose that the broad overlap of values between patients and controls in the previous studies concerning the predictive value of soluble CD31 levels (36–39) was caused by circulating CD31 represents a mixture of the transmembraneless and truncated forms; in addition, it was not possible, until now, to discriminate between the two soluble forms of CD31. In a therapeutic perspective, it is therefore necessary to find alternative strategies to rescue CD31-mediated T cell regulation in situations in which pathogenic T cells have already undergone activation and CD31 shedding.

Zehnder et al. (26) reported that the presence of Abs targeting the 23 juxta-membrane amino acid sequence of CD31 (LYP21) inhibited the MLR in a specific and dose-dependent manner. Intriguingly, a synthetic 23-mer peptide corresponding to the epitope of the LYP21 Ab (aa 551–574) equally inhibited MLRs, which showed dispersed small aggregates of cells, rather than the single large aggregate observed in control MLRs (26). Therefore, it appears that the CD31 peptide is able to reproduce the physiologic active detachment signal, which is mutually driven in live leukocytes by CD31–CD31 interactions (6). However, stimulated T cells typically lose CD31 at their surface (13) and Zehnder et al. (26) demonstrated that the peptide was effective also on CD31-negative enriched T cells. As a consequence, the mechanism involved in the immunosuppressive effect exerted by the CD31 peptide 551–574 was left unresolved.

The present study demonstrates that the extracellular portion of CD31 recognized by MBC 78.2/PECAM-1.2 Ab (domain 6) (23), which is located on the N-terminal of the aa 551–574 (26), remains expressed on CD31^{shed} T cells. We have also documented that the CD31 551–574 immunosuppressive peptide is highly homophilic; therefore, we hypothesized that it can homo-oligomerize with the truncated CD31 on CD31^{shed} cells and thus act by mimicking the second step of the CD31 homophilic engagement described by Newton et al. (33): the *cis*-homo–dimerization of the molecule. Indeed, the analysis of the CD31 domain 6 distribution showed that the peptide clusters localize between the CD31 domain 6 clusters. We thus postulate that the peptide rescues the CD31–ITIM inhibitory signaling in CD31^{shed} T cells by bridging the distant truncated CD31 molecules over the cell surface. This hypothesis is supported by the fact that either Ab-mediated CD31 domain 6 crosslinking or treatment with the CD31 551–574 peptide durably enhanced the phosphorylation of CD31 ITIMs and SHP2 and inhibited TCR-induced activation and proliferation of T cells in vitro. Based on the data, we cannot rule out that the peptide clusters might exert other effects in T cells. Of note, we also show that the CD31 peptide inhibits Ag-induced T cell responses in vivo (in the delayed type hypersensitivity model), pointing to a potential immunosuppressive therapeutic effect for this peptide in chronic inflammatory diseases.

We demonstrate that, upon cell activation, the loss of T cell CD31 is due to its cleavage and shedding of the truncated portion of its ectodomain into biologic fluids. CD31 shedding results in the loss of its inhibitory function, as the necessary *trans*-homophilic engagement of the molecule cannot be established by CD31^{shed} cells because they lack the distal Ig-like domain 1. However, *cis*-homo–oligomerization, which is induced by the *trans*-homophilic engagement of the molecule, is the key event in CD31 inhibitory signal transduction. Therefore, it is possible to use a homophilic peptide or an appropriate peptidomimetic compound to mimic the *cis*-homo–oligomerization step and rescue the lost physiologic immunoregulatory function of CD31 on activated T cells. Such a therapeutic approach might be useful for treating debilitating chronic immunoinflammatory diseases in which CD31 signaling is suspected to play an important protective role, such as in rheumatoid arthritis (9), multiple sclerosis (8), inflammatory liver disease (40), and atherothrombosis (24, 27, 41).

Acknowledgments

We thank Dr. Mary Osborne-Pellegrin (INSERM U698) and Dr. Frans Nauwelaers (BD Biosciences Europe, Scientific Affairs, Erembodegem, Belgium) for help editing the manuscript, Sébastien Lacroix-Desmazes (INSERM U872) for help with the BIAcore analysis, and Pascal Roux (Plate forme d'imagerie dynamique-Imagopole, Institut Pasteur, Paris, France) for the TIRF acquisition.

Disclosures

The authors have no financial conflicts of interest.

References

1. Newman, P. J. 1999. Switched at birth: a new family for PECAM-1. *J. Clin. Invest.* 103: 5–9.
2. Newman, P. J., M. C. Berndt, J. Gorski, G. C. White, II, S. Lyman, C. Paddock, and W. A. Muller. 1990. PECAM-1 (CD31) cloning and relation to adhesion molecules of the immunoglobulin gene superfamily. *Science* 247: 1219–1222.
3. Muller, W. A., S. A. Weigl, X. Deng, and D. M. Phillips. 1993. PECAM-1 is required for transendothelial migration of leukocytes. *J. Exp. Med.* 178: 449–460.
4. Bird, I. N., J. H. Spragg, A. Ager, and N. Matthews. 1993. Studies of lymphocyte transendothelial migration: analysis of migrated cell phenotypes with regard to CD31 (PECAM-1), CD45RA and CD45RO. *Immunology* 80: 553–560.
5. Tada, Y., S. Koarada, F. Morito, O. Ushiyama, Y. Haruta, F. Kanegae, A. Ohta, A. Ho, T. W. Mak, and K. Nagasawa. 2003. Acceleration of the onset of collagen-induced arthritis by a deficiency of platelet endothelial cell adhesion molecule 1. *Arthritis Rheum.* 48: 3280–3290.
6. Brown, S., I. Heinisch, E. Ross, K. Shaw, C. D. Buckley, and J. Savill. 2002. Apoptosis disables CD31-mediated cell detachment from phagocytes promoting binding and engulfment. *Nature* 418: 200–203.
7. Newton-Nash, D. K., and P. J. Newman. 1999. A new role for platelet-endothelial cell adhesion molecule-1 (CD31): inhibition of TCR-mediated signal transduction. *J. Immunol.* 163: 682–688.
8. Graesser, D., A. Solowiej, M. Bruckner, E. Osterweil, A. Juedes, S. Davis, N. H. Ruddle, B. Engelhardt, and J. A. Madri. 2002. Altered vascular permeability and early onset of experimental autoimmune encephalomyelitis in PECAM-1-deficient mice. *J. Clin. Invest.* 109: 383–392.
9. Wong, M. X., J. D. Hayball, P. M. Hogarth, and D. E. Jackson. 2005. The inhibitory co-receptor, PECAM-1 provides a protective effect in suppression of collagen-induced arthritis. *J. Clin. Immunol.* 25: 19–28.
10. Goel, R., B. R. Schrank, S. Arora, B. Boylan, B. Fleming, H. Miura, P. J. Newman, R. C. Molthen, and D. K. Newman. 2008. Site-specific effects of PECAM-1 on atherosclerosis in LDL receptor-deficient mice. *Arterioscler. Thromb. Vasc. Biol.* 28: 1996–2002.
11. Stockinger, H., W. Schreiber, O. Majdic, W. Holter, D. Maurer, and W. Knapp. 1992. Phenotype of human T cells expressing CD31, a molecule of the immunoglobulin supergene family. *Immunology* 75: 53–58.
12. Thiel, A., J. Schmitz, S. Miltenyi, and A. Radbruch. 1997. CD45RA-expressing memory/effector Th cells committed to production of interferon-gamma lack expression of CD31. *Immunol. Lett.* 57: 189–192.
13. Demeure, C. E., D. G. Byun, L. P. Yang, N. Vezzio, and G. Delespesse. 1996. CD31 (PECAM-1) is a differentiation antigen lost during human CD4 T-cell maturation into Th1 or Th2 effector cells. *Immunology* 88: 110–115.
14. Kohler, S., and A. Thiel. 2009. Life after the thymus: CD31+ and CD31- human naive CD4+ T-cell subsets. *Blood* 113: 769–774.
15. Goldberger, A., K. A. Middleton, J. A. Oliver, C. Paddock, H. C. Yan, H. M. DeLisser, S. M. Albelda, and P. J. Newman. 1994. Biosynthesis and processing of the cell adhesion molecule PECAM-1 includes production of a soluble form. *J. Biol. Chem.* 269: 17183–17191.
16. Zehnder, J. L., K. Hirai, M. Shatsky, J. L. McGregor, L. J. Levitt, and L. L. Leung. 1992. The cell adhesion molecule CD31 is phosphorylated after cell

activation. Down-regulation of CD31 in activated T lymphocytes. *J. Biol. Chem.* 267: 5243–5249.
17. Ilan, N., A. Mohsenin, L. Cheung, and J. A. Madri. 2001. PECAM-1 shedding during apoptosis generates a membrane-anchored truncated molecule with unique signaling characteristics. *FASEB J.* 15: 362–372.
18. Yun, P. L., A. A. Decarlo, C. C. Chapple, and N. Hunter. 2005. Functional implication of the hydrolysis of platelet endothelial cell adhesion molecule 1 (CD31) by gingipains of Porphyromonas gingivalis for the pathology of periodontal disease. *Infect. Immun.* 73: 1386–1398.
19. Garton, K. J., P. J. Gough, J. Philalay, P. T. Wille, C. P. Blobel, R. H. Whitehead, P. J. Dempsey, and E. W. Raines. 2003. Stimulated shedding of vascular cell adhesion molecule 1 (VCAM-1) is mediated by tumor necrosis factor-alpha-converting enzyme (ADAM 17). *J. Biol. Chem.* 278: 37459–37464.
20. Mendez, M. P., S. B. Morris, S. Wilcoxen, E. Greeson, B. Moore, and R. Paine, III. 2006. Shedding of soluble ICAM-1 into the alveolar space in murine models of acute lung injury. *Am. J. Physiol. Lung Cell. Mol. Physiol.* 290: L962–L970.
21. Eugenin, E. A., R. Gamss, C. Buckner, D. Buono, R. S. Klein, E. E. Schoenbaum, T. M. Calderon, and J. W. Berman. 2006. Shedding of PECAM-1 during HIV infection: a potential role for soluble PECAM-1 in the pathogenesis of NeuroAIDS. *J. Leukoc. Biol.* 79: 444–452.
22. Fawcett, J., C. Buckley, C. L. Holness, I. N. Bird, J. H. Spragg, J. Saunders, A. Harris, and D. L. Simmons. 1995. Mapping the homotypic binding sites in CD31 and the role of CD31 adhesion in the formation of interendothelial cell contacts. *J. Cell Biol.* 128: 1229–1241.
23. Yan, H. C., J. M. Pilewski, Q. Zhang, H. M. DeLisser, L. Romer, and S. M. Albelda. 1995. Localization of multiple functional domains on human PECAM-1 (CD31) by monoclonal antibody epitope mapping. *Cell Adhes. Commun.* 3: 45–66.
24. Caligiuri, G., E. Groyer, J. Khallou-Laschet, A. Al Haj Zen, J. Sainz, D. Urbain, A. T. Gaston, M. Lemitre, A. Nicoletti, and A. Lafont. 2005. Reduced immunoregulatory CD31+ T cells in the blood of atherosclerotic mice with plaque thrombosis. *Arterioscler. Thromb. Vasc. Biol.* 25: 1659–1664.
25. In vivo assays for lymphocyte function. 2001. *In Current Protocols in Immunology.* Shevach, E. M., J. E. Coligan, B. Bierer, and D. H. Margulies. John Wiley & Sons. Unit 4.5.
26. Zehnder, J. L., M. Shatsky, L. L. Leung, E. C. Butcher, J. L. McGregor, and L. J. Levitt. 1995. Involvement of CD31 in lymphocyte-mediated immune responses: importance of the membrane-proximal immunoglobulin domain and identification of an inhibiting CD31 peptide. *Blood* 85: 1282–1288.
27. Caligiuri, G., P. Rossignol, P. Julia, E. Groyer, D. Mouradian, D. Urbain, N. Misra, V. Ollivier, M. Sapoval, P. Boutouyrie, et al. 2006. Reduced immunoregulatory CD31+ T cells in patients with atherosclerotic abdominal aortic aneurysm. *Arterioscler. Thromb. Vasc. Biol.* 26: 618–623.
28. Chen, Y., P. G. Schlegel, N. Tran, D. Thompson, J. L. Zehnder, and N. J. Chao. 1997. Administration of a CD31-derived peptide delays the onset and significantly increases survival from lethal graft-versus-host disease. *Blood* 89: 1452–1459.
29. Muller, W. A., M. E. Berman, P. J. Newman, H. M. DeLisser, and S. M. Albelda. 1992. A heterophilic adhesion mechanism for platelet/endothelial cell adhesion molecule 1 (CD31). *J. Exp. Med.* 175: 1401–1404.
30. Vernon-Wilson, E. F., F. Auradé, and S. B. Brown. 2006. CD31 promotes beta1 integrin-dependent engulfment of apoptotic Jurkat T lymphocytes opsonized for phagocytosis by fibronectin. *J. Leukoc. Biol.* 79: 1260–1267.
31. Wong, C. W., G. Wiedle, C. Ballestrem, B. Wehrle-Haller, S. Etteldorf, M. Bruckner, B. Engelhardt, R. H. Gisler, and B. A. Imhof. 2000. PECAM-1/CD31 trans-homophilic binding at the intercellular junctions is independent of its cytoplasmic domain; evidence for heterophilic interaction with integrin alphavbeta3 in Cis. *Mol. Biol. Cell* 11: 3109–3121.
32. Sachs, U. J., C. L. Andrei-Selmer, A. Maniar, T. Weiss, C. Paddock, V. V. Orlova, E. Y. Choi, P. J. Newman, K. T. Preissner, T. Chavakis, and S. Santoso. 2007. The neutrophil-specific antigen CD177 is a counter-receptor for platelet endothelial cell adhesion molecule-1 (CD31). *J. Biol. Chem.* 282: 23603–23612.
33. Newton, J. P., C. D. Buckley, E. Y. Jones, and D. L. Simmons. 1997. Residues on both faces of the first immunoglobulin fold contribute to homophilic binding sites of PECAM-1/CD31. *J. Biol. Chem.* 272: 20555–20563.
34. Couty, J. P., C. Rampon, M. Leveque, M. P. Laran-Chich, S. Bourdoulous, J. Greenwood, and P. O. Couraud. 2007. PECAM-1 engagement counteracts ICAM-1-induced signaling in brain vascular endothelial cells. *J. Neurochem.* 103: 793–801.
35. Newman, P. J., and D. K. Newman. 2003. Signal transduction pathways mediated by PECAM-1: new roles for an old molecule in platelet and vascular cell biology. *Arterioscler. Thromb. Vasc. Biol.* 23: 953–964.
36. Khare, A., S. Shetty, K. Ghosh, D. Mohanty, and S. Chatterjee. 2005. Evaluation of markers of endothelial damage in cases of young myocardial infarction. *Atherosclerosis* 180: 375–380.
37. Wei, H., L. Fang, S. H. Chowdhury, N. Gong, Z. Xiong, J. Song, K. H. Mak, S. Wu, E. Koay, S. Sethi, et al. 2004. Platelet-endothelial cell adhesion molecule-1 gene polymorphism and its soluble level are associated with severe coronary artery stenosis in Chinese Singaporean. *Clin. Biochem.* 37: 1091–1097.
38. Kuenz, B., A. Lutterotti, M. Khalil, R. Ehling, C. Gneiss, F. Deisenhammer, M. Reindl, and T. Berger. 2005. Plasma levels of soluble adhesion molecules sPECAM-1, sP-selectin and sE-selectin are associated with relapsing-remitting disease course of multiple sclerosis. *J. Neuroimmunol.* 167: 143–149.
39. Figarella-Branger, D., N. Schleinitz, B. Boutière-Albanèse, L. Camoin, N. Bardin, S. Guis, J. Pouget, C. Cognet, J. F. Pellissier, and F. Dignat-George. 2006. Platelet-endothelial cell adhesion molecule-1 and CD146: soluble levels and in situ expression of cellular adhesion molecules implicated in the cohesion of endothelial cells in idiopathic inflammatory myopathies. *J. Rheumatol.* 33: 1623–1630.
40. Goel, R., B. Boylan, L. Gruman, P. J. Newman, P. E. North, and D. K. Newman. 2007. The proinflammatory phenotype of PECAM-1-deficient mice results in atherogenic diet-induced steatohepatitis. *Am. J. Physiol. Gastrointest. Liver Physiol.* 293: G1205–G1214.
41. Groyer, E., A. Nicoletti, H. Ait-Oufella, J. Khallou-Laschet, A. Varthaman, A. T. Gaston, O. Thaunat, S. V. Kaveri, R. Blatny, H. Stockinger, et al. 2007. Atheroprotective effect of CD31 receptor globulin through enrichment of circulating regulatory T-cells. *J. Am. Coll. Cardiol.* 50: 344–350.